Advanced numerical investigation into structural behaviour of high strength cold-formed steel lapped Z-sections with different overlapping lengths

H C Ho and *K F Chung

Department of Civil and Environmental Engineering, The Hong Kong Polytechnic University, Hung Hom, Kowloon, Hong Kong SAR, PR China.

Abstract

In order to improve buildability of cold-formed steel structures, a series of research and development projects have been undertaken by the authors to examine structural behaviour of bolted moment connections between cold-formed steel sections. In this paper, a systematic numerical investigation with advanced finite element modelling technique into the structural behaviour of high strength cold formed steel lapped Z-sections under gravity loads is presented, and details of the modelling techniques are presented thoroughly. It aims to examine deformation characteristics of these lapped Z-sections with different overlapping lengths. After careful calibration of advanced finite element models of lapped Z-sections against test data, it is demonstrated that the predicted moment rotation curves of these models follow closely the measured data not only up to the maximum applied moments, but also at large deformations. In general, all of these lapped Z-sections are unable to resist sustained loadings after section failure under combined bending and shear, and they exhibit sudden unloadings once the maximum applied loads are attained. Hence, the proposed finite element models are able to simulate highly non-ductile deformation characteristics of these Z-sections.

While long overlapping lengths over internal supports in multi-span cold-formed steel purlin systems are often advantageous in terms of both 'stiffness and strength', more steel materials are used at the same time. Hence, it is very desirable to establish an efficient use of the lapped Z-sections with optimal overlapping lengths. A total of 6 models with different overlapping lengths are then extended to simulate the structural behaviour of lapped double span beams, and extensive material and geometrical non-linear analyses have been carried out. It is found that lapped double span beams with practical overlapping lengths tend to behave superior to continuous double span beams in terms of both load resistances and deformations. Depending on the overlapping lengths of the lapped Z-sections, different system failure mechanisms have been clearly identified after significant moment redistribution within the beams, and their structural behaviour have been compared in a

rational manner. Consequently, these models will be readily employed to investigate the structural behaviour of high strength cold-formed steel lapped Z-sections under a wide range of practical loading and boundary loading conditions for possible development of effective design rules.

Key words: Cold-formed steel Z-sections, lapped Z-sections, finite element analysis, combined bending and shear, non-ductile deformations

1. Introduction

Over the last three decades, thin gauge steel strips account for over 50% of the annual production of many steel producers in the world. A significant portion of these steel strips are rolled into cold-formed steel sections and sheetings which are adopted widely used in construction due to their excellent structural efficiency, high versatility in applications and good buildability in construction. Nowadays, cold-formed steel construction has grown into a multi-billon US dollar industry of building products throughout the world.

One of the common applications of the cold-formed steel sections is to act as purlins in metal building envelopes which support metal roof and wall claddings against both gravity and wind loads. Owing to their simply geometries and ease of installation, both C- and Z-sections are commonly used. The depths of these sections typically range from 150 to 350 mm while their thicknesses typically range from 1.2 to 3.2 mm. The yield strengths of the sections are 280 and 350 N/mm^2. In the recent years, high strength cold-formed steel sections with yield strengths at 450 N/mm^2 are also available which provide engineered purlin systems with high load carrying capacities. These sections are attached to metal claddings through various types of fixings to form effective roof and wall systems. Although design rules on their use may be found in various technical recommendations (EN 1993-1-3:2006, AISI S100-07.), full scale tests on these sections together with fixings and claddings are usually required to assess their performance under both gravity and wind loads (Johnson and Hancock 1994; Hancock *et al.* 2001; Murray and Elhouar 1994; Toma and Wittemann 1994) in order to attain high structural efficiency. In general, understanding to the structural behaviour of these purlin and roof systems is extremely important as it is very common to have the same design and construction used repeatedly in millions of tons of cold-formed steel sections and claddings.

In general, owing to its member configuration, the structural performance of a cold-formed steel purlin system supporting a modern metal roof system (Willis and Wallace 1990; Chung and St Quinton 1996; Yu 2010) is affected by the following restraints:

- intermittent lateral and twisting restraints offered by a roof system at the top flange of the purlin along its member length,
- discrete lateral restraints offered by secondary bracing members to the web of the purlin at intermediate positions along its member length, and
- lateral and rotational restraints offered within the lapped sections of the purlin at purlin-rafter connections over supports.

Owing to the co-existence of these restraints in the roof system, their combined effects are readily quantified in full-scale system tests, but difficult to be itemized individually. Hence, any change in materials, dimensions and arrangements of cold-formed steel sections and sheetings often require a complete set of full-scale system tests to be carried out for verification and validation on their structural performance (Chung and St Quinton 1996; Zhang and Tong 2008). This is very time-consuming and expensive.

It should be noted that in modern building envelopes with metal roof and wall claddings, many components are specifically designed or modified to satisfy various architectural, thermal and water-tightness requirements, and their structural forms are often hampered by the need to accommodate other components and their installation sequences. In the recent years, a large number of modern building envelopes with metal roof and wall claddings have been developed for buildings in which concealed fixings with halters are adopted. These concealed fixings are often developed in such a way to allow the cladding systems to attain high functional performance on water tightness and thermal insulation, etc., and this often leads to significant penalty in the structural performance (Chung and St Quinton 1996; Yu 2010). Hence, the moment resistances of these cold-formed steel purlin members depend significantly on the levels of restraints offered by various attached claddings and other elements of roof systems. Consequently, it is highly desirable to develop scientific tools to assess structural behaviour of cold-formed steel purlin members, and the effects of various restraining effects onto the load-deformation characteristics of the purlin members should be properly accounted for.

In this paper, a systematic numerical investigation with advanced finite element modelling technique into the structural behaviour of cold formed steel lapped Z-sections is presented. It aims to examine deformation characteristics of these lapped Z-sections with different overlapping lengths.

1.1. Previous investigation on structural stability of purlin members

In general, cold-formed steel sections are open and thin sections which are torsionally weak and highly susceptible to lateral instability. Owing to the geometry of cold-formed steel sections, their structural performance is very different to those of hot-rolled steel I-sections and channels (Hancock, Murray and Ellifritt 2001; Yu 2010):

i) in a C-section, the shear centre of the cross-section does not coincide with its centriod, and thus, it is normally subjected to combined bending and torsion in the presence of lateral loads; and
ii) in a Z-section, the principal axes of the cross-section do not coincide with their centroidal axes, and thus, it is normally subjected to bi-axial bending in the presence of lateral loads.

A comprehensive test series of cold-formed steel C-sections under combined bending and torsion was reported by Put *et al.* (1999). A complementary numerical study was also reported by Pi *et al.* (1998), and a realistic finite element model was developed to investigate the elastic lateral-distortional buckling, the inelastic behaviour, and the moment resistances of C-sections in the presence of residual stresses and initial imperfections. The effects of moment distribution and load height on the lateral-distortional buckling resistances were also studied. Similar investigations on the lateral instability of cold-formed steel Z-sections under bi-axial bending were also reported by Put *et al.* (1999). However, it should be noted that the dimensions of these C-sections are rather small, i.e. 102 mm (D) x 53 mm (B) x 1.0 or 1.9 mm (t), and it is necessary to extend these models to incorporate practical loading conditions in purlin systems in which the actions of the wind loads are applied through claddings, and then through different attachments and fixings, such as halters and screws, onto the top flanges of these sections.

1.2 Previous investigation on structural stability of purlin systems

It is essential to investigate into lateral instability of partially restrained cold-formed steel purlin systems in which loads are applied to top flanges of the sections in the presence of

different restraining effects offered by various components in the roof systems. Hence, both the support and the restraint conditions of these sections should be properly incorporated into analysis and design.

It should be noted that the beneficial effects of intermittent lateral restraints provided by attached roof claddings have been long identified, and the mechanism is well understood (Chung and St Quinton 1996; Gao and Moen 2012; Gajdzicki and Goczek 2015; Ghosn and Sinno 1996; Hancock *et al.* 1993; Rousch and Hancock 1997; Toma and Wittemann 1994). Many attempts have been made over the years to incorporate this effect to increase the load carrying capacities of purlin members with some success. The effect of discrete lateral restraints provided by secondary bracing members is often simplified by assigning full positional restraints to the purlin members during numerical modelling. Such simplification may be adopted in practice although these secondary bracing members may not be fully effective due to lack-of-fit, bolt slippage, misalignment, or even buckling under compression. Moreover, the benefits of strength and stiffness enhancement in the overlapped sections over internal supports and of reduced unrestrained lengths of the Z-sections are often neglected for simplicity. Hence, the effect of the longitudinal rotational restraints offered by lapped Z-sections at purlin-rafter connections are often simplified conservatively. Only continuous sections are incorporated instead by some researchers (Lucas *et al.* 1997a, 1997b).

In order to promote the effective use of cold-formed steel sections in building construction, a series of research and development projects have been undertaken by the authors to study the structural behaviour of multi-span purlin systems using high strength cold-formed steel sections with overlaps. It should be noted that over the years, six test series with a total of 26 single point load tests on lapped Z-sections were carried out to investigate the structural behaviour of the lapped Z-sections (Ho and Chung 2004), and the test results have been successfully employed to evaluate the effective flexural rigidities, EI_{eff} , of lapped Z-sections with bolted moment connections of different configurations (Chung and Ho 2005). Hence, adoption of the effective flexural rigidities of these lapped Z-sections over internal supports enables rational design of high strength cold-formed steel multi-span purlin systems under both gravity and wind loads (Ho and Chung 2006). Consequently, it is considered to be highly beneficial to develop effective numerical models on both continuous Z-sections and lapped Z-sections with various overlapping lengths in order to analyse their structural

behaviour with sufficient structural adequacy. The numerical results will be readily adopted for subsequent development of rational design rules.

1.3 Failure mechanism of fully restrained multi-span purlin systems

According to both experimental and numerical investigations carried out by the authors (Chung and St Quinton 1996; Chung 2004), it was proposed that typical failure mechanism of a fully restrained double span purlin system using continuous Z-sections may be divided into the following stages, as shown in Figure 1:

- *Linear elastic stage*

  Under a small applied load, w kN/m, the purlin system behaves in a linear elastic manner. As the applied load increases, the corresponding hogging moment over the internal support reaches the section failure resistance of the Z-section under combined bending and shear. The first 'partial strength hinge' is then formed.

- *Non-linear stage with moment redistribution*

  Upon further increase in the applied load, the purlin system undergoes a non-linear deformation with significant moment redistribution, and a large rotational deformation of the purlin will take place over the internal support according to the residual moment resistance of the failed Z-section. Hence, the applied moment over the internal support will be readily distributed towards the mid-span of each purlin member until formation of the second 'partial strength hinge'.

- *System failure with large deformation*

  During moment redistribution, the purlin system will act partially as a double simply supported beam with a residual moment resistance over the internal support under any additional load. System failure will take place when the maximum sagging moment near mid-span of the purlin member reaches the moment resistance of the Z-section.

However, few experimental investigations into the structural behaviour of lapped double span purlin systems were found in the literature. While the overall deformation characteristics of a lapped double span purlin system is expected to follow broadly to those of a double span

purlin system with continuous purlin sections, the effect of lapped Z-sections with different overlapping lengths should be quantified experimentally and numerically.

It should be noted that the term 'partial strength hinge' is adopted above instead of the term 'plastic hinge' because of lack of rotational ductility in cold-formed steel Z-sections.

1.4 Finite element modelling

A number of finite element models on cold-formed steel and stainless steel sections have been reported in the literature (Ashrafa *et al.* 2006; Bakker and Pekoz 2003; Chung 2004; Dinis and Camotim 2010; Li 2004; Lucas *et al.* 1997a, 1997b; Telue and Mahendran 2004; Ye *et al.* 2004; Zhou and Young 2007;) over the years with different levels of detailing and accuracy on element formulations, material models, cross-section definitions, and mesh configurations. Moreover, various methods on detailed modelling on both support and loading conditions of purlin systems using C- and Z-sections have been proposed, depending on availability of suitable finite elements and computing resources. Experiences and in-sights from these researchers in finite element modelling have been studied carefully for possible adoption in the present study.

In general, the thin degenerated 4 noded shell element, namely, Element S4R, is commonly employed by many researchers in their finite element models to examine the structural behaviour of cold-formed steel sections against various interactive modes of local buckling, distortional buckling as well as overall lateral buckling. However, most of these studies are found to focus on the structural behaviour of these sections under their maximum loads while little effort is made to examine their post buckling behaviour at large deformations.

2. Objectives and scope of work

In order to improve buildability of cold-formed steel structures, a series of research and development projects have been undertaken by the authors to examine structural behaviour of various forms of bolted moment connections between cold-formed steel sections. It should be noted that six test series with a total of 26 single point load tests on lapped cold-formed steel Z sections were carried out by the authors to investigate structural behaviour of the lapped connections. Full details of the experimental investigation may be found in the literature (Ho and Chung 2004; Chung and Ho 2005).

In this paper, a systematic numerical investigation with advanced finite element modelling technique into the structural behaviour of cold formed steel lapped Z-sections is presented. It aims to examine deformation characteristics of these lapped Z-sections with different overlapping lengths. As a whole, the numerical investigation takes the following forms of activities:

a) to establish finite element models of lapped Z-sections with different overlapping lengths under single point loads;
b) to calibrate these models against test results of the test series mentioned above;
c) to develop finite element models of lapped double span purlin systems using cold-formed steel Z-sections with different overlapping lengths; and
d) to examine structural behaviour of the purlin systems, identify various modes of failure, and determine structural advantages of these systems over purlin systems with continuous Z-sections.

The areas of interest in this numerical investigation include:

- detailed modelling of the overlapping zone (with contact elements) of lapped Z-sections;
- section failure of Z-sections under combined bending and shear;
- load deflection curves of lapped Z-sections, especially at large deformations; and
- overall structural behaviour of lapped double span purlin systems, in particular, moment re-distribution over internal supports.

3. Reference tests

A total of six tests on pairs of simply supported Z-sections with different overlapping lengths are adopted in the present study as reference tests for calibration of the proposed finite element models (Ho and Chung 2004). In all these tests, a generic lipped Z-section is adopted which is commonly referred as Section Z15016 G450. It should be noted that Section Z15016 denotes a lipped Z-section with a section depth of 150 mm and a thickness of 1.6 mm, and G450 denotes a nominal yield strength at 450 N/mm^2. Table 1 summarizes the test programme and the measured cross-sectional dimensions of the Z-sections together with measured mechanical properties of the steel materials.

Figure 2 illustrates a typical test set-up of the single point load tests on the lapped Z-sections. It is shown that in each test, a pair of nominally identical Z-sections are tested in a simply supported condition under an applied load at mid-span. In order to provide restraints to the Z-sections, steel strips are provided as interconnections to the Z-sections at regular intervals, and they are connected to both the top and the bottom flanges of the sections with screws. Moreover, wooden blocks are also provided between the section webs, and they are securely attached with screws. The load is applied directly to the webs of the Z-sections through bolts.

The maximum applied load, the observed mode of failure and the corresponding deformation characteristics of each of the tests are presented in Table 2. It should be noted that in all tests, section failure of the Z-sections under combined bending and shear is observed, as shown in Figure 3. The moment rotation curves obtained from the tests are presented in Figure 4 for easy reference. In general, all of these curves show a sudden unloading after section failure. Hence, the lapped Z-sections are unable to resist sustained loadings, and they exhibit highly non-ductile deformation characteristics after section failure.

It should be noted that the observed mode of failure may be generally described as a combination of the following:

i) local buckling in the plate element of the cross-section under compression
ii) distortional buckling in the cross-section under bending, and
iii) overall lateral and twisting deformation of the member under combined bi-axial bending and torsion.

Owing to the presence of the interconnections provided at regular intervals along the spans of the Z-sections, lateral and twisting deformations of the Z-sections at the interconnections is effectively eliminated while local buckling and cross-sectional distortional buckling in the Z-sections between the interconnections are apparent. The levels of restraint provided to the Z-sections in the tests are adopted for calibration of the proposed finite element models.

4. Finite element modelling

The general finite element package, ABAQUS (Version 6.13), is adopted in this study, and advanced finite element models with both material and geometric non-linearity (ABAQUS

2013; Young and Yan, 2002; Ashrafa *et al.* 2006; Bakker and Pekoz 2003; Chung 2004; Telue and Mahendran 2004) are established to simulate the deformation characteristics of lapped Z-sections with different overlapping lengths. Figure 5a) illustrates typical finite element models of the lapped Z-sections with Sections Z15016 G450 under the test conditions respectively. It should be noted that different types of finite elements are employed to model the Z-sections, the interconnections, the screw fixings as well as the interfaces between the Z-sections and the interconnections. Key features of the finite element models are described as follows:

a) Material model

As shown in Figure 5c), a bi-linear stress strain curve according to the measured mechanical properties of the Z-sections is adopted in the numerical analyses. It should be noted that

i) both the yield strength and the Young's modulus were obtained from standard coupon tests on steel strips cut from the webs of the Z-sections, and the material properties of these steel sections are presented in Table 1; and

ii) for simplicity, the effect of residual stresses in the cross-sections in both flat elements and rounded corners due to cold working are neglected. Nevertheless, the yield strengths of the rounded corners in the cross-sections are assigned to be 1.05 p_y, where p_y is the measured yield strength of the Z sections. In general, these two effects are considered to have relatively minor effects on the buckling behaviour of the Z-sections.

b) Shell element

In order to simulate both in-plane and out-of-plane deformations of the Z-sections undergoing significant material yielding and geometrical buckling, a continuum 8 noded shell element, namely SC8R, as shown in Figure 5b), is adopted in the present study owing to its good structural accuracy at large deformations. It should be noted that

i) as each node has three translational degrees of freedom, the total degrees of freedom in one element is thus 24. Unlike a conventional shell element which discretizes a reference surface, this element discretizes an entire three-dimensional body with its full geometry specified by the co-ordinates of the nodes;

ii) the effects of transverse shear deformation and thickness change have been fully incorporated into the formulation of the element for accurate prediction of finite membrane deformations and large rotations; and

iii) as the element may readily be stacked to provide more refined through-thickness responses, it allows accurate prediction on transverse forces as well as through-thickness pinching forces.

Thus, the element is highly appropriate for non-linear three-dimensional geometric analyses of thin-walled sections under both in-plane and out-of-plan loadings. Figure 5d) illustrates the definitions of the cross-sections of the Z-sections using shell element SC8R, and it should be noted that two elements are used to model the round corners of the cross-sections as trimmed corners for simplicity.

c) Loading and support conditions

A typical finite element model is shown in Figure 6a), and it should be noted that

i) the lapped Z-sections are supported with fixed supports at their left ends, and roller supports at their right ends, and these boundary conditions are applied to the bottom flanges of the Z-sections at supports rather than at their mid-height in order to correspond directly to the test conditions;

ii) the applied load in each model, i.e. the total applied load, is taken as 2P, and hence, the applied load to each of the Z-sections is P only; the applied load is then further divided into 4 quarters, i.e. 4 nos. of P / 4, and each of them is shared equally to all the nodes around a bolt hole in the section web through a set of 'radial' springs; all of these springs are assigned to have a high compressive stiffness at 1,000 kN/mm, but a low tensile stiffness at 0.001 N/mm. The use of the 'radial' springs allows consistent load distribution among all the nodes around the bolt holes in the section webs; local bearing deformation in the webs around the bolt holes is not modelled in the present investigation for simplicity; and

iii) lateral restraints are provided as interconnections to both the top and the bottom flanges of the sections, and typical values of the restraint stiffnesses given in the literature (Fan *et al.* 1997; Rogers and Hancock 1999) is adopted.

d) Modelling of overlapping zones

In order to model accurately the overlapping zones of the Z-sections, the contact areas between the Z-sections are carefully modelled (Zhou and Young 2007) as shown in Figure 6b), as follows:

i) contacts between the cross-sections of the Z-sections within the overlapping zones are modelled with 'radial' spring elements, namely, SPRING2, with a high compressive stiffness at 1,000 kN/mm, but a low tensile stiffness at 0.001 N/mm, so that mesh intrusion is prevented effectively; and

ii) a high compressive force will be induced only in the pre-defined direction of the spring element during deformation, and hence, no force will be induced in any other direction.

During the model development, a number of advanced contact elements have been employed to model the contact surfaces. However, it is found that in some cases, numerical convergence is difficult to achieve as there are a large number of contact elements in the overlapping zones which may undergo various possible deformations during iterations, leading to numerical instability. Instead, the use of spring elements is found to be very successful in eliminating numerical instability during analyses of the lapped Z-sections.

e) Finite element mesh

The finite element mesh of the lapped Z-section under a simply supported condition is illustrated in Figure 6a). In order to establish a finite element model with optimal structural accuracy and numerical efficiency, a sensitivity exercise on the mesh configurations was carried out. The mesh adopted for the present study shown in Figure 6a) comprises of a total of 36,318 nodes and 18,108 elements. It should be noted that

i) the element size is typically 10 x 25 mm^2 and 12.5 x 25 mm^2 for the flange and the web elements of the Z-sections respectively, and thus, the aspect ratios of these elements are successfully kept between 2.0 and 2.5; and

ii) the mesh is refined locally in the mid-span regions of the Z-sections as well as at the points of interconnection so that the aspect ratios of these elements are kept between 1.0 and 1.25.

f) Modelling of bolted interconnections

In order to model accurately the bolted connections of the Z-sections within the overlapping zone, the bolted connections are carefully modelled, as shown in Figure 6c), as follows:

i) all the bolted connections are modelled with spring elements of different stiffnesses along three perpendicular directions, namely, k_{ix} , k_{iy} and k_{iz}, which are estimated by the load-bearing deformation characteristics of the bolted connection as shown in Figure 6c).

ii) the load-deformation characteristics of the bolted connections may be well described with the use of α_b which is a non-linear function of a bearing deformation, δ_o ; and

iii) the values of various translational restraints are adopted from the test results of various lapped shear tests of screwed connections with steel strips of different thicknesses and yield strengths reported in the literature (Chung and Ip 2000).

g) Initial geometrical imperfection

In general, it is necessary to provide initial geometrical imperfections in the models to facilitate smooth transition across bifurcation limits during equilibrium iterations in order to avoid numerical divergence. Although this is not necessary in the present case as the Z-sections will deflect laterally and twist longitudinally under bi-axial bending and torsion, it is considered to be appropriate to incorporate initial geometrical imperfections into the models as part of a standard procedure of numerical modelling. Hence, elastic linear eigenvalue analyses on the Z-sections under single point loads at mid-span are performed, and the deformed mode shapes at first bifurcation, i.e. the eigenmodes corresponding to the lowest eigenvalues, are extracted. The eigenmodes are then superimposed to the perfect geometries of the Z-sections as initial geometrical imperfections, and the magnitude of the maximum out-of-plane initial imperfections is taken to be 0.25 t, where t is the thickness of the Z-sections. The initial geometrical imperfections of typical models are illustrated in Figure 7.

5. Calibration of finite element models

It should be noted that a total of six models with different overlapping lengths have been established, and material and geometrical non-linearity analyses in all these models has been successfully completed. Typical deformed shapes of the models under the maximum applied moments are illustrated in Figure 7. The failure mode of the lapped Z-sections may be well described as interactive local plate buckling and cross-sectional distortional buckling near the end of the overlapping zone. Moreover, deformed shapes of both models at large deformations are also presented in Figure 7, and extensive plastic buckling in the Z-sections near mid-span is apparent. These are found to correspond closely to the observed deformations of the Z-sections in the tests after failure.

Both the measured and the predicted moment rotation curves of each of the six tests are plotted onto the same graphs in Figure 8 for easy comparison. It is demonstrated that the predicted moment rotation curves of these models follow closely the measured data not only up to the maximum applied moments, but also at large deformations. Hence, the highly non-ductile deformation characteristics of these lapped Z-sections have been successfully captured with the models.

5.1 Model factors

Table 3 summarizes both the measured and the predicted moment resistances of the six lapped Z-sections. In order to access structural accuracy of the models, a model factor, MF, is established which is defined as follows:

$$MF = M_{test} / M_{FEM}$$

where

M_{test} is the measured moment resistance of a lapped Z-section obtained from a test, and

M_{FEM} is the predicted moment resistance of the corresponding finite element model of the lapped Z-section.

It should be noted that the value of MF should be larger than unity if the model is conservative, i.e. the predicted moment resistance is smaller than the measured value. In general, the values of MF should range from 1.0 to 1.2 for conservative and yet efficient

models. All the model factors for the finite element models are summarized in Table 3 for easy comparison. It is shown that the model factors in assessing the moment resistances of all the six models are found to range from 0.97 to 1.06 with an average value of 1.03. Moreover, for those finite element models with practical overlapping lengths, i.e. Models ZA030R, ZA060R and ZA090R, together with the model of the control test, i.e. Model ZACON, the average model factor is 1.04. Hence, all these models are considered to be effective in predicting the structural behaviour of the Z-sections at failure.

6. Modelling of double span purlin systems

While long overlapping lengths over internal supports in multi-span cold-formed steel purlin systems are often advantageous in terms of both 'stiffness and strength', more steel materials are used at the same time. Hence, it is essential to establish an efficient use of the lapped Z-sections with optimal overlapping lengths. This is readily achieved through a comprehensive comparison among the deformation characteristics of various models.

6.1 Double span beam models

In order to examine the structural performance of multi-span cold-formed steel purlin systems under gravity loads, a total of six different double span beam models with Section Z15016 G450 have been established as follows:

- Continuous beam model

  There is only one model in which the Z-section is continuous over the internal support, and it is refereed as Model DSB. The finite element mesh together with the loading and boundary conditions of the double span system is shown in Figure 9a). The deformation characteristics of the model may be readily taken as a reference when assessing those of the models with various overlapping lengths.

- Lapped beam models

  Five different double span beam models have been established which overlapping lengths are taken as 4D, 5D, 6D, 7D and 8D (where D is the depth of the Z-section), and they are referred as Models DSB-4D, DSB-5D, DSB-6D, DSB-7D and DSB-8D.

Typical mesh together with the loading and boundary conditions of the double span system is shown in Figure 9b).

It should be noted that

- Lateral restraints, k_d , are provided at regular intervals to the top flanges of the models, as shown in Figure 9, and these two restraints are readily offered to the Z-sections by attached roof claddings in practical purlin-supported roof systems. Typical value of these restraints at 5.0 kN/mm provided at an interval of 200 mm along the beam span (Fan *et al.* 1997; Rogers and Hancock 1999) is adopted in the present study.

- Full lateral restraints are also provided at one third span of the Z-sections according to common practice in cold-formed steel purlin systems, as shown in Figure 9, and their presence has significant effects on lateral stability of the Z-sections whenever compression flanges of these Z-sections are unrestrained.

6.2 Data analysis

In general, owing to the highly non-ductile deformation characteristic of the lapped Z-sections after section failure, significant moment redistribution within the models take place, leading to some degrees of difficulty in numerical convergence. Nevertheless, all the models for both continuous and lapped double span beams have been successfully analysed under gravity loads. Typical deformed shapes of Models DSB, DSB-4D, DSB-6D and DSB-8D, are shown in Figures 10 to 13 respectively while those of Models DSB-5D and DSB-7D are not shown for simplicity. It should be noted that:

- Model DSB

  As shown in Figure 10, the first ‘partial strength hinge’ in this model is formed at the cross-section directly over the internal support as both applied hogging moments and shear forces attain their maximum values. Owing to significant reduction in the moment resistance of the Z-section at large rotations, moment redistribution takes place sharply within the beam, and two additional ‘partial strength hinges’ are formed near the mid-span of each of the span of the beam, leading to a systematic three-hinge mechanism.

- Model DSB-4D

  In this model, as the moment resistance of the lapped Z-section has been significantly increased because of overlapping, the first 'partial strength hinge' cannot form at the lapped section over the internal support, as shown in Figure 11. Instead, the first 'partial strength hinge' is formed in the single Z-section close to one end of the lapped sections, i.e. the critical single section, at which both the applied moment and shear force have only been reduced by a small extent, when compared with their maximum values at the internal support. As the applied load increases, moment redistribution takes place sharply within the beam owing to highly non-ductile deformation characteristics of the Z-sections after section failure with a small residual moment resistance at large rotations. An additional 'partial strength hinge' is then formed near the mid-span of any one span of the beam, leading to an unsymmetrical system failure.

- Models DSB-6D and DSB-8D

  Owing to the presence of long overlapping lengths, the failure mechanism of Models DSB-6D and DSB-8D is very different from that of Model DSB-4D. As the single sections of the lapped beam models are far away from the internal supports, both the applied moment and shear forces at the ends of the overlapped zones have been substantially reduced. Hence, the first 'partial strength hinges' will not take place at the critical single sections, and instead, they form in the lapped sections directly over the internal supports, as shown in Figures 12 and 13. As the applied loads increase, moment redistribution takes place gradually within the beams, and an additional 'partial strength hinge' is then formed near the mid-span of any one span of the beams, leading also to an unsymmetrical system failure.

Figure 14 plots the load deflection curves of all the six models onto the same graph for direct comparison while Table 4 summarizes the applied loads corresponding to various stages of deformations in both the continuous and the lapped beam models.

It should be noted that

- In Model DSB, the first 'partial strength hinge' is formed when the applied load, w, reaches 2.59 kN/m. After significant moment redistribution, the second 'partial strength hinge' is formed when the applied load, w, reaches 4.12 kN/m. It should be

noted that there is a significant increase in the beam deflection associated with the formation of the second 'partial strength hinge' because of a significant reduction in both the residual moment resistance and the flexural rigidity of the Z-section directly over the internal support.

- In all the lapped beam models, the first 'partial strength hinges' are formed when the applied load, w, reaches a value ranging from 4.49 to 5.45 kN/m. These are well above that of Model DSB at 2.59 kN/m. Moreover, all the lapped beam models allow significant moment redistribution during formation of the second 'partial strength hinges', and the corresponding applied load, w, ranges from 4.79 to 5.37 kN/m.

- In general, for all lapped beam models considered in this section, they behave superior to the continuous beam model in terms of both load resistances and deformations, as demonstrated in the load deflection curves. Moreover, Model DSB-7D is shown to be the most effective among all the six models in terms of resistance, deformation and use of steel materials.

7. Conclusions

In this paper, a systematic numerical investigation with advanced finite element modelling technique into the structural behaviour of cold formed steel lapped Z-sections with different overlapping lengths is presented. Advanced finite element models with material and geometrical non-linearity are established to simulate the deformation characteristics of a total of six lapped Z-sections with different overlapping lengths. After incorporating carefully the interconnections provided at regular intervals along the spans of the Z-sections, the models have been successfully calibrated against test data. It is demonstrated that the predicted moment rotation curves of these models follow closely the measured data not only up to the maximum applied moment, but also at large deformations.

In order to examine the structural performance of multi-span cold-formed steel purlin systems under gravity loads, these advanced models have been extended into lapped double span beams with five different overlapping lengths directly over internal supports. Lateral restraints are provided to the Z-sections according to common practice while typical magnitudes of these restraints are adopted in the present study.

It is shown that

- Advanced finite element models have been established to simulate successfully the structural behaviour of lapped Z-sections under single point loads, and they are demonstrated to be effective in simulating full range deformation characteristics of lapped Z-sections under combined bending and shear, including the highly non-ductile deformation characteristics after section failure.

- Moreover, lapped double span beams with practical overlapping lengths tend to behave superior to continuous double span beams in terms of both load resistances and deformations. Depending on the overlapping lengths of the lapped sections, the first 'partial strength hinge' may occur at the single sections near the ends of the overlapping zones, or at the lapped sections directly over the internal supports. After significant moment redistribution, the second 'partial strength hinge' is formed near the mid-span of any span of the beam, forming an unsymmetrical system mechanism.

- Various restraints have been carefully incorporated into the finite element models according to common practice in modern roof structures while the magnitudes of these restraints depend on specific connection details adopted. These restraints are very important as they affect the structural behaviour of the models significantly. While typical values adopted in the present study are presented in Section 4, measured data of these restraints should be obtained directly in tests, wherever possible.

- 'Radial' spring elements are provided onto contact surfaces within the overlapping zones of the lapped Z-sections as their use often render a robust model which achieves numerical convergence readily, when compared with modern surface elements which may cause numerical instability at large deformations.

- Owing to the complexity of the problems, the present investigation is by no means exhaustive. Other key parameters with significant effects on the structural behaviour of lapped Z-sections in double or multi-span beams, such as the ratio of the overlapping length to the beam span, are not included. Hence, similar to many other finite element studies, key findings of the finite element models are problem-specific, and they should only be generalized with cautions. Nevertheless, it is demonstrated that the proposed finite element models are able to provide accurate prediction to the structural behaviour of double span or multi-span lapped Z-sections.

It should be noted that this study is part of an extensive experimental and numerical investigation into the structural behaviour of multi-span purlin systems using high strength cold-formed steel Z-sections with overlaps. The proposed models will be extended to investigate the structural behaviour of high strength cold-formed steel lapped Z-sections under a wide range of beam spans, and practical boundary and loading conditions which will be reported in a separate paper.

ACKNOWLEDGEMENT

The research project leading to the publication of this paper is supported by the Research Grants Council of the Government of the Hong Kong Special Administrative Region (Project No. PolyU5149/10E).

REFERENCES

ABAQUS. ABAQUS Analysis User's Manual, Vol. I – X. Version 6.13. ABAQUS Theory Manual Version 6.13. Providence, RI, USA: Dassault Systèmes Simulia Corp, 2013.

AISI S100-07. 2007. North American Specifications for the Design of Cold-Formed Steel Structural Members, America Iron and Steel Institute; 2007.

Ashrafa M, Gardner L and Nethercot D A. Finite element modelling of structural stainless steel cross-sections. Thin-Walled Structures. 2006; 44:1048–1062.

Bakker MCM and T. Pekoz T. The finite element method for thin-walled members - Basic principles. Thin-Walled Structures. 2003; 41: 179–189.

Chung KF and St Quinton D. Structural performance of modern roofs with thick over-purlin insulation – Experimental investigation. Journal of Constructional Steel Research. 1996; 40(1):17-38.

Chung KF and Ip KH. Finite element modeling of bolted connections between cold formed steel strips and hot rolled steel plates under static shear loading. Engineering Structures 2000; 22(10):1271-1284.

Chung KF. Investigations into cold-formed steel structures with bolted moment connections. Proceedings of the International Symposium on Cold-formed Metal Structures. Hong Kong. 10 December 2004, pp41-66.

Chung KF and Ho HC. Structural behaviour of high strength cold-formed steel Z purlins with overlaps. Proceedings of the Seventeenth International Specialty Conference on Cold-formed Steel Structures, Orlando, Florida; November 2004, 777-800.

Chung KF and Ho HC. Analysis and design of lapped connections between cold-formed steel Z sections. Thin-Walled Structures. 2005; 43(7):1071-1090.

Dinis PB and Camotim D. 2010. Local/distortional mode interaction in cold-formed steel lipped channel beams. Thin-Walled Structures, 48 (10-11): 771-785.

Eurocode 3. BS EN 1993-1-3:2006. Design of steel structures. Part 1.3: General rules – Supplementary rules for cold-formed members and sheeting. British Standards Institution; 2006.

Fan LX, Rondal J and Cescotto S. Numerical simulation of lap screw connections. Thin-Walled Structures. 1997; 29 (1-4): 235-241.

Gao T, and Moen C. Predicting rotational restraint provided to wall girts and roof purlins by through-fastened metal panels. Thin-Walled Structures. 2012; 61:145-153.

Gajdzicki M, and Goczek J. Numerical determination of rotational restraint of cold-formed Z-purlin according to EC3. International Journal of Steel Structures. 2015; 3:633-645.

Ghosn A and Sinno R. Load capacity of nested, laterally braced, cold-formed steel Z-section beams. Journal of Structural Engineering. 1996; 122(8):968-971.

Hancock GJ, Celeban M and Healy C. Behaviour of purlins with screw fastened sheeting under wind uplift and downwards loading, Australian Civil Engineering Transaction. 1993; 35(3): 221-233.

Hancock GJ, Murray TM, Ellifritt DS. Cold-formed steel structures to the AISI specification, New York: Marcel Dekker, 2001.

Ho HC and Chung KF. Experimental investigation onto the structural behaviour of lapped connections between cold-formed steel Z sections. Thin-Walled Structures. 2004; 42:1013-1033.

Ho HC and Chung KF. Analytical prediction on deformation characteristics of lapped connections between cold-formed steel Z sections. Thin-Walled Structures. 2006; 44(1): 115-130.

Johnston N. and Hancock G.J. Calibration of the AISI R-factor design approach for purlins using Australian test data, Engineering Structures, 1994;16(5): 342-347.

Murray TM and Elhouar S. North American approach to the design of continuous Z- and C- purlins for gravity loading with experimental verification. Engineering Structures. 1994; 16(5):337-341.

Li LY. Lateral–torsional buckling of cold-formed zed-purlins partial-laterally restrained by metal sheeting. Thin-Walled Structures. 2004;42(7): 995-1011.

Lucas RM, Al-Bermani FGA and Kitipornchai S. Modelling of cold-formed purlin-sheeting systems. Part 1: Full model. Thin-Walled Structures. 1997; 27:223–243.

Lucas RM, Al-Bermani FGA and Kitipornchai S. Modelling of cold-formed purlin-sheeting systems. Part 2: Simplified model. Thin-Walled Structures. 1997; 27: 263–286.

Pi LY, Put BM and Trahair NS. Lateral buckling strengths of cold-formed channel section beams. Journal of Structural Engineering. 1998; 124:1182-1191.

Put BM, Pi LY and Trahair NS. Bending and torsion of cold-formed channel beams. Journal of Structural Engineering. 1999; 125: 540-546.

Put BM, Pi LY and Trahair NS. Biaxial bending of cold-formed Z-beams. Journal of Structural Engineering. 1999; 125: 1284-1290.

Rogers C A. and Hancock G J. Screwed connection tests on thin G550 and G300 sheet steels. Journal of Structural Engineering. 1999; 125:128-136.

Rousch CJ and Hancock GJ. Comparison of tests of bridged and unbridged purlins with a non-linear analysis model. Journal of Constructional Steel Research. 1997; 41(2-3): 197-220

Telue Y and Mahendran M. Numerical modelling and design of unlined cold-formed steel wall frames. Journal of Constructional Steel Research, 2004; 60: 1241-1256.

Toma T and Wittemann K. Design of cold-formed purlins and rails restrained by sheeting. Journal of Constructional Steel Research. 1994; 31: 149-168.

Willis CT and Wallace B. Behavior of cold-formed steel purlins under gravity loading. Engineering Structures. 1990; 116(8):2061-2069.

Ye ZM, Kettle R, and Li LY. Stress analysis of cold-formed zed purlins partially restrained by steel sheeting. Computers and Structures. 2004; 82(9): 731-739.

Young B and Yan J. Finite element analysis and design of fixed-ended plain channel columns. Finite Elements in Analysis and Design 2002; 38(6):549–66.

Yu W W. Cold-formed steel design, Fourth Edition, New York, Chichester: Wiley, 2010.

Zhang L, Tong G. Moment resistance and flexural rigidity of lapped connections in multi-span cold-formed Z purlin systems. Thin-Walled Structures. 2008;46(5):551-560

Zhou F, Young B. Experimental and numerical investigations of cold-formed stainless steel tubular sections subjected to concentrated bearing load. Journal of Constructional Steel Research 2007;63(11):1452-1466.

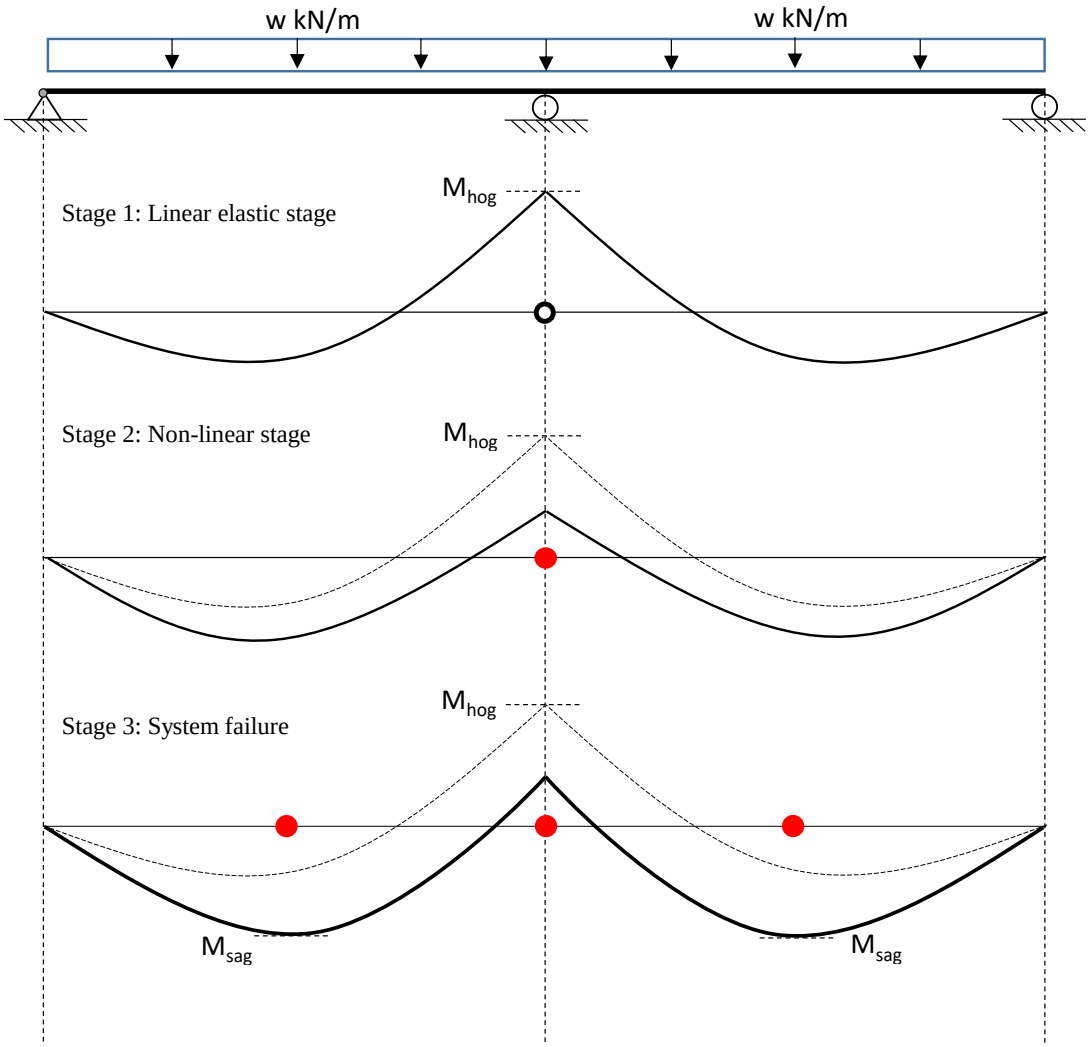

Figure 1. Failure mechanism of a continuous double span purlin system

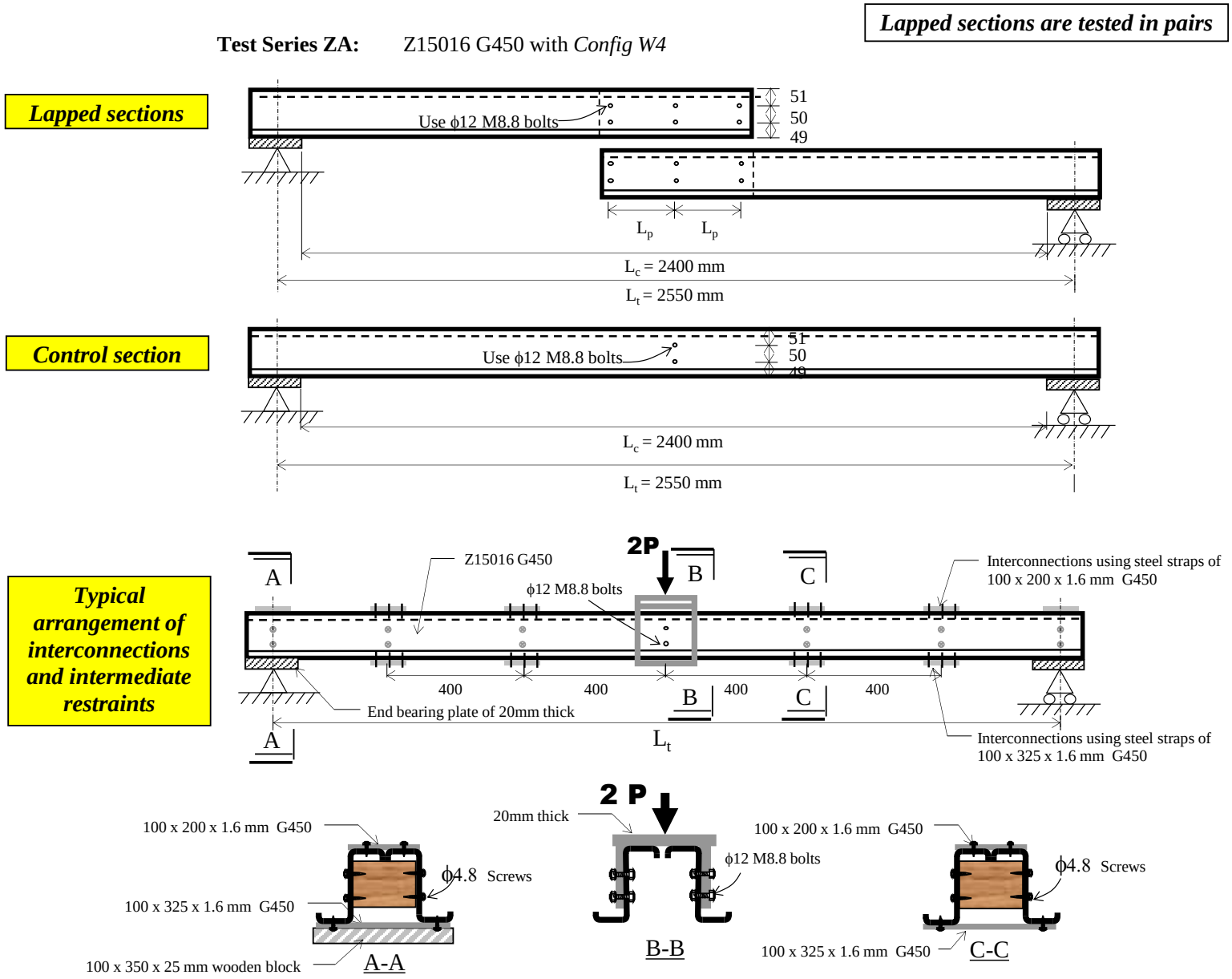

Figure 2. Typical set-up of single point load tests on lapped Z-sections

a) Test ZACONR

Section failure under combined bending and shear near mid-span

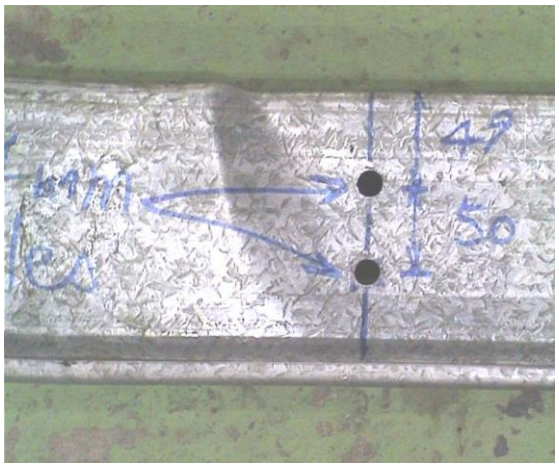

A close-up view on failed section (after the test)

b) Test ZA090R

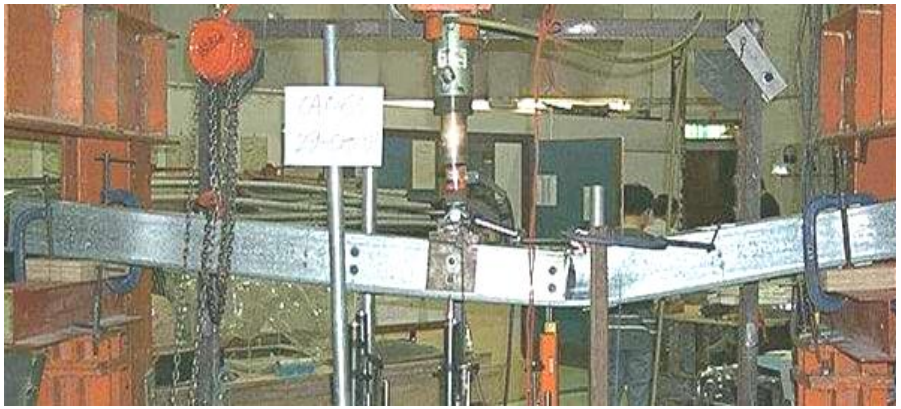

Section failure under combined bending and shear at the end of lap

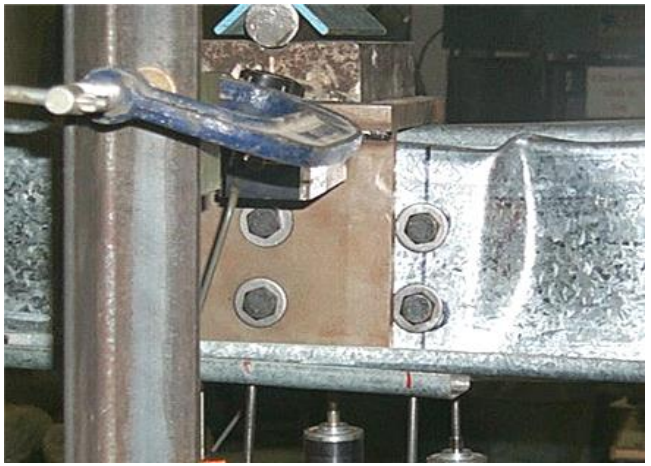

A close-up view on failed section (after the test)

Figure 3. Various modes of failure in single point load tests on lapped Z sections

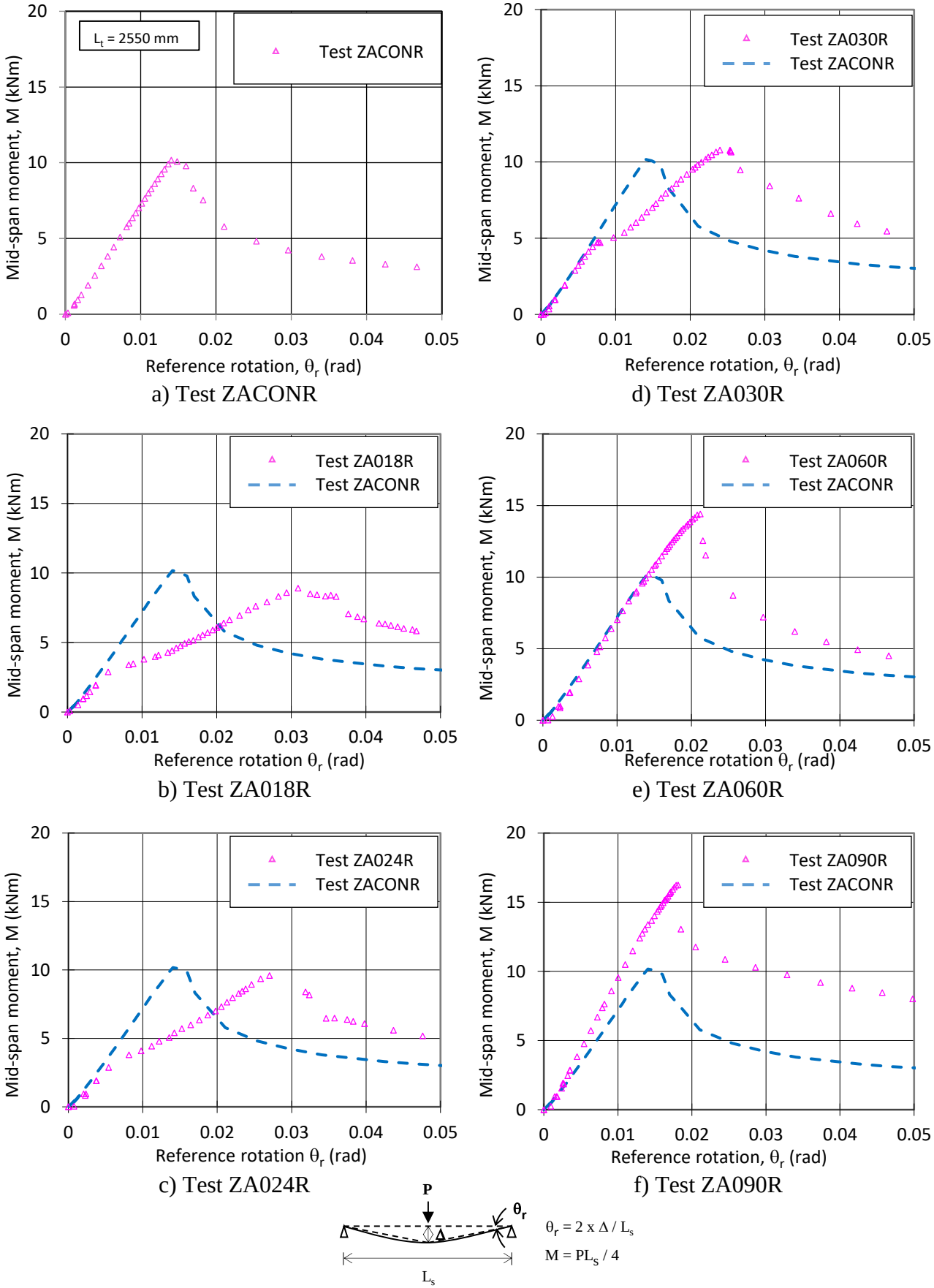

Figure 4. Measured moment rotation curves of single point load tests on lapped sections

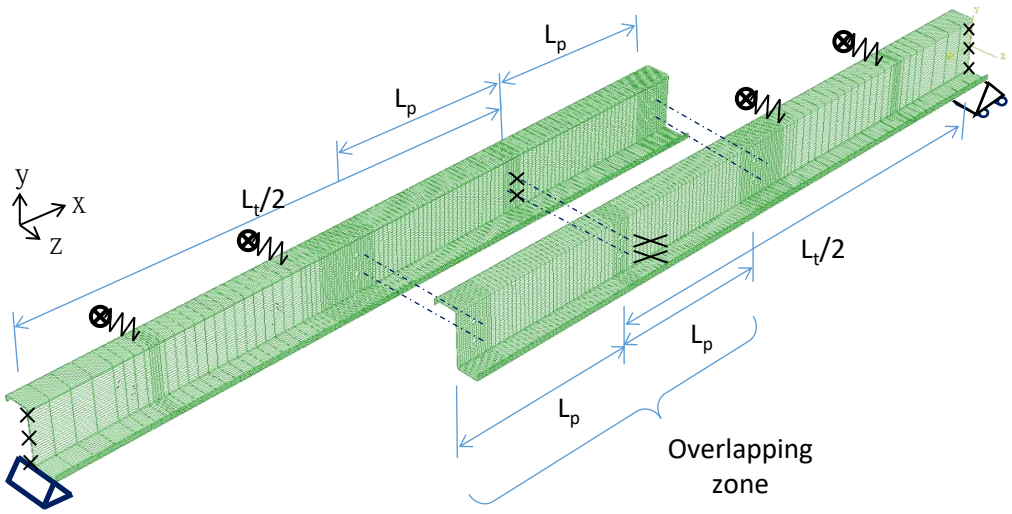

a) Typical finite element model layout of lapped Z sections

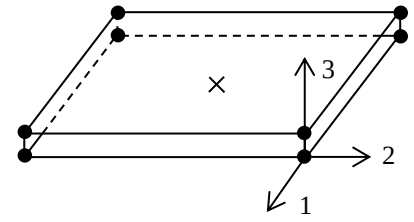

× Integration point

Continuum 8 noded shell model
The full 3-D geometry is specified, and the element thickness is defined by the nodal geometry.

Degrees of freedom
u_1, u_2, u_3

Total degree of freedom = 8 x 3 = 24

The integration point is located at the centroid of the element.

b) Details of shell element SC8R

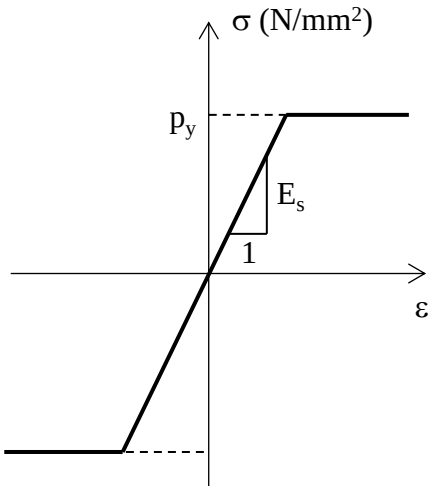

c) Idealized bi-linear stress strain curve

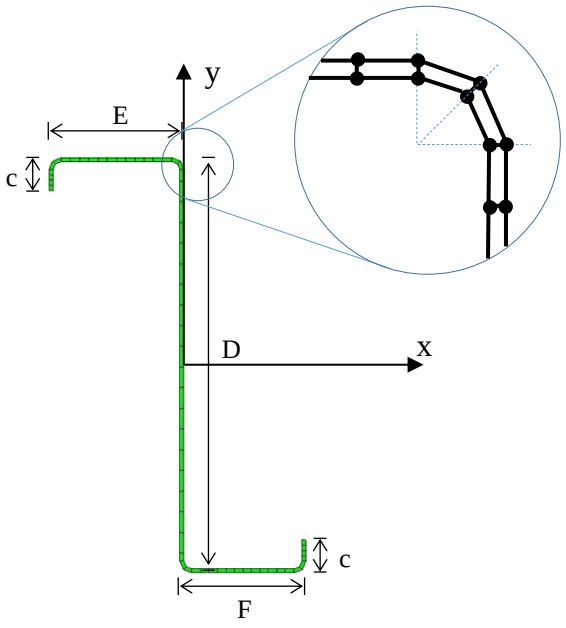

d) Definitions of the cross section of a Z-section

Figure 5. Typical finite element model of lapped Z sections under single point loads

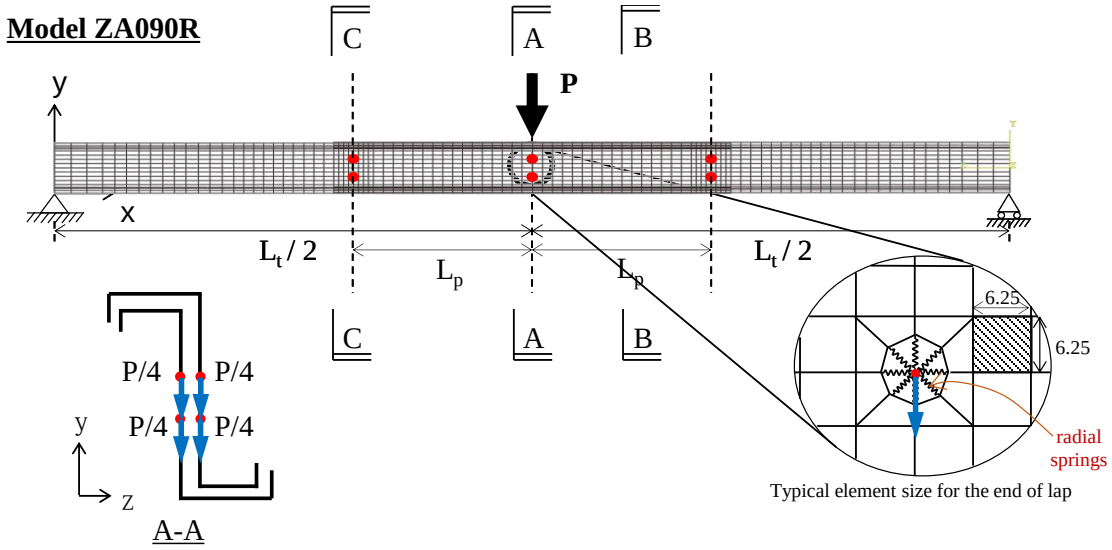

a) Overall layout and meshing of lapped sections

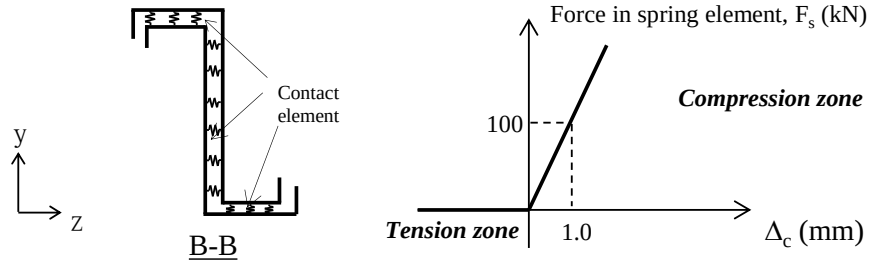

b) Details of contact properties between the lapped Z sections over the entire overlapping zone

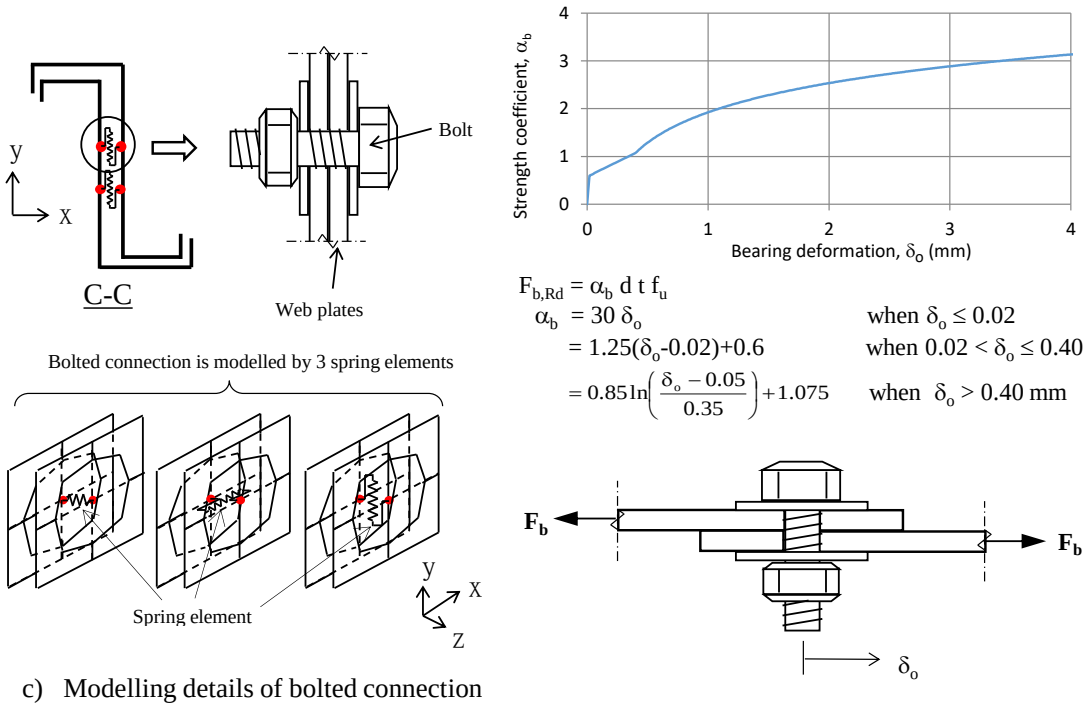

c) Modelling details of bolted connection

Figure 6 Details of loading and boundary conditions of finite element models of lapped Z sections

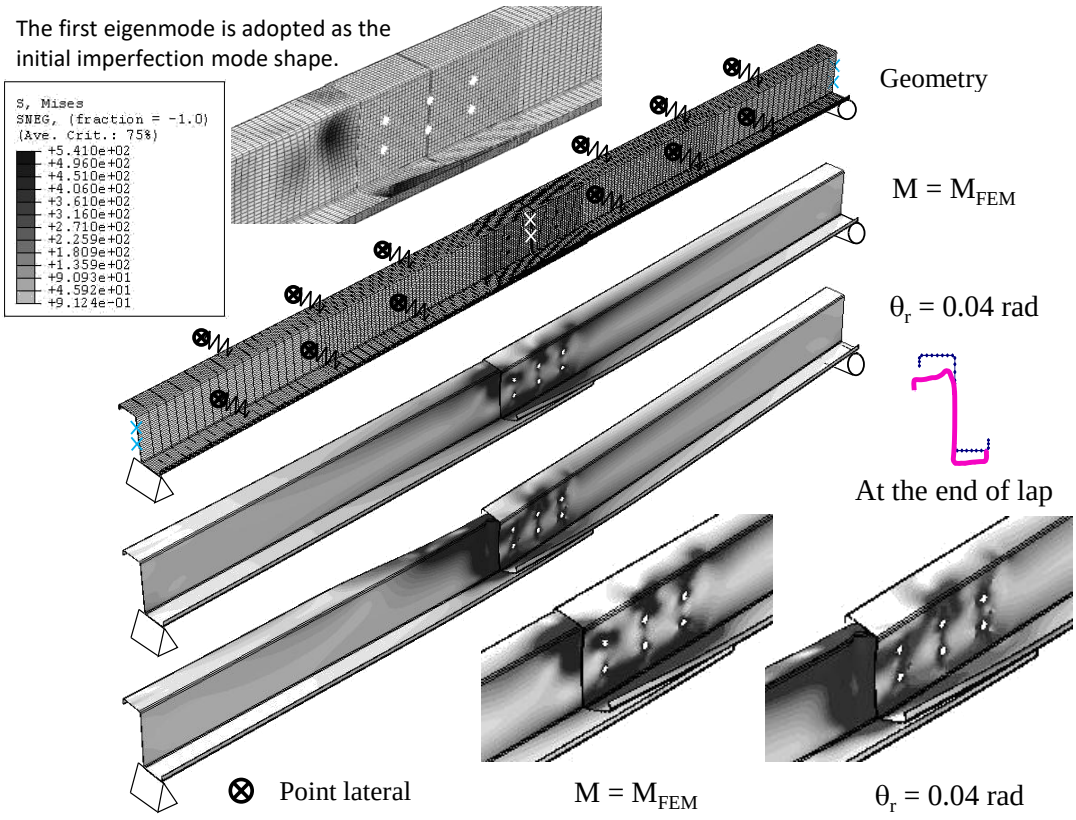

a) Finite element mesh and deformed shapes of Model ZA018R under various applied loads

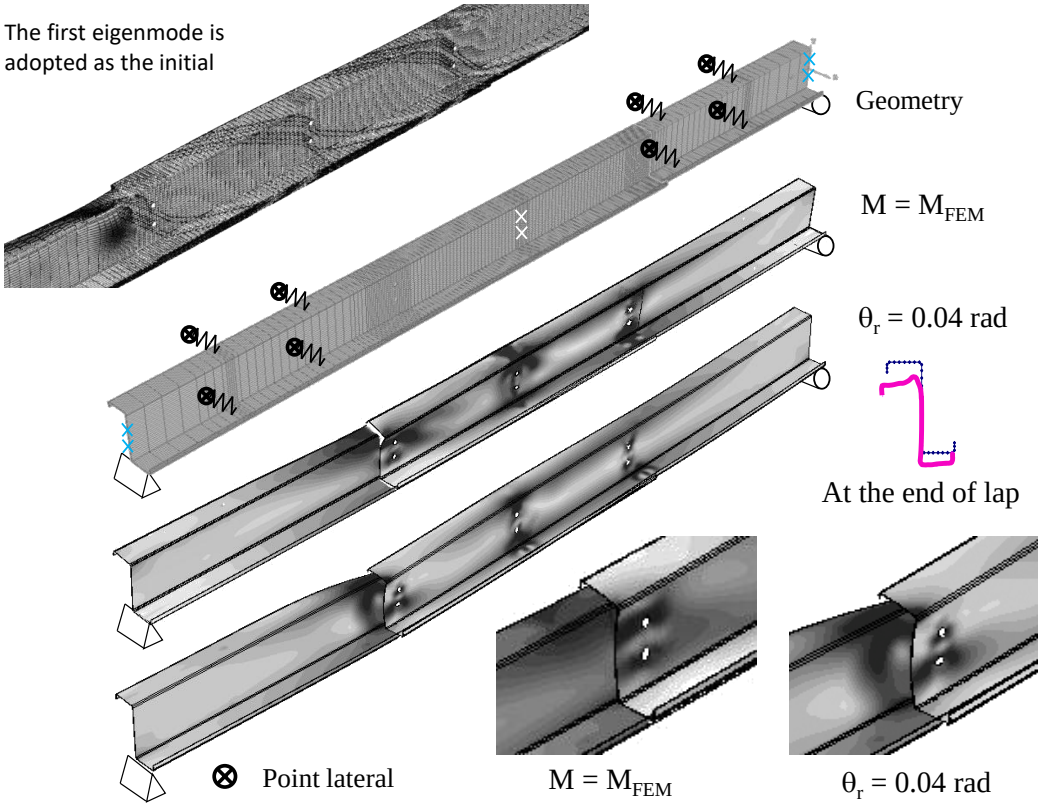

b) Finite element mesh and deformed shapes of Model ZA090R under various applied loads

Figure 7. Numerical analyses and results of Models ZA018R and ZA090R

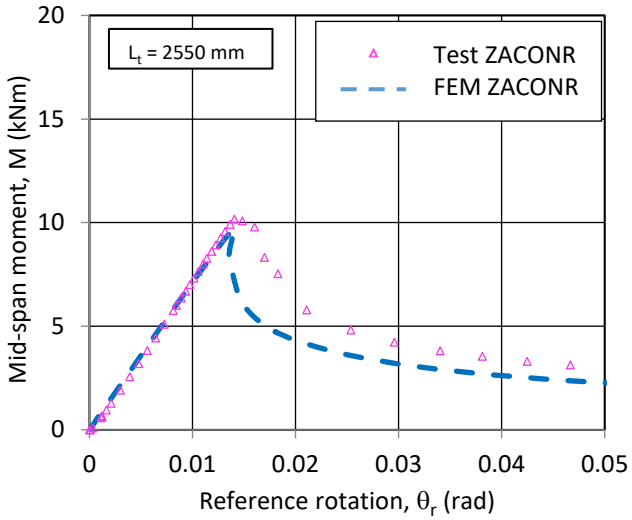

a) Test ZACONR

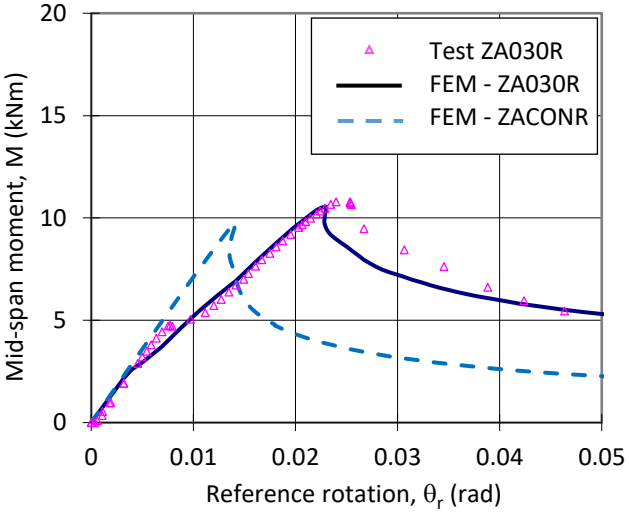

d) Test ZA030R

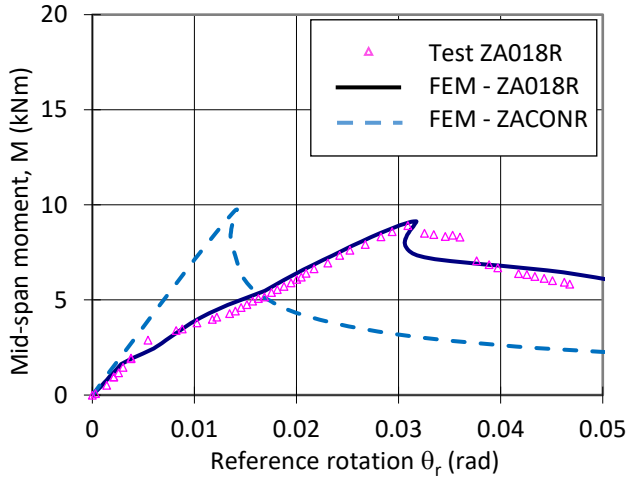

b) Test ZA018R

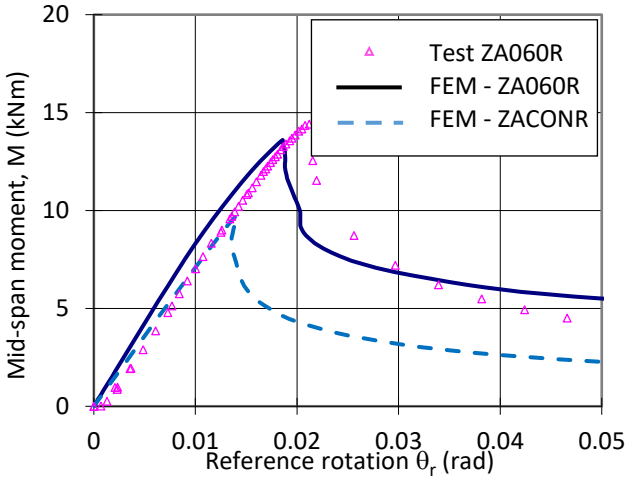

e) Test ZA060R

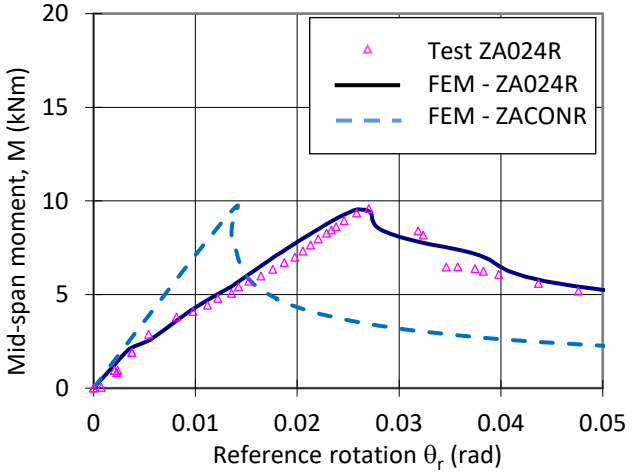

c) Test ZA024R

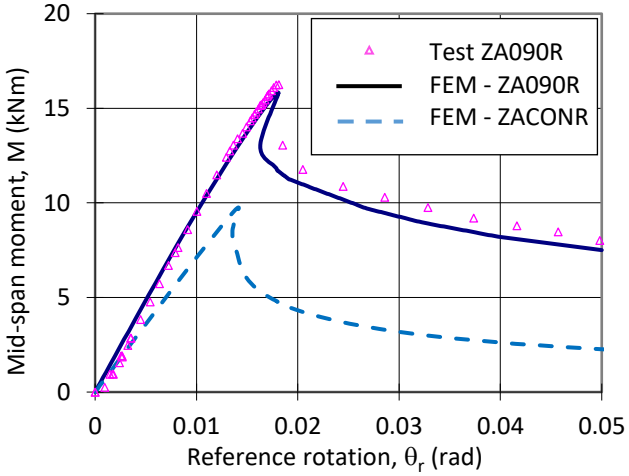

f) Test ZA090R

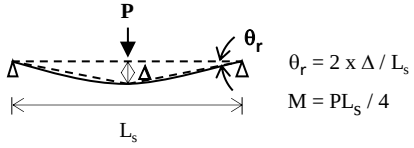

Figure 8. Moment rotation curves of lapped Z sections

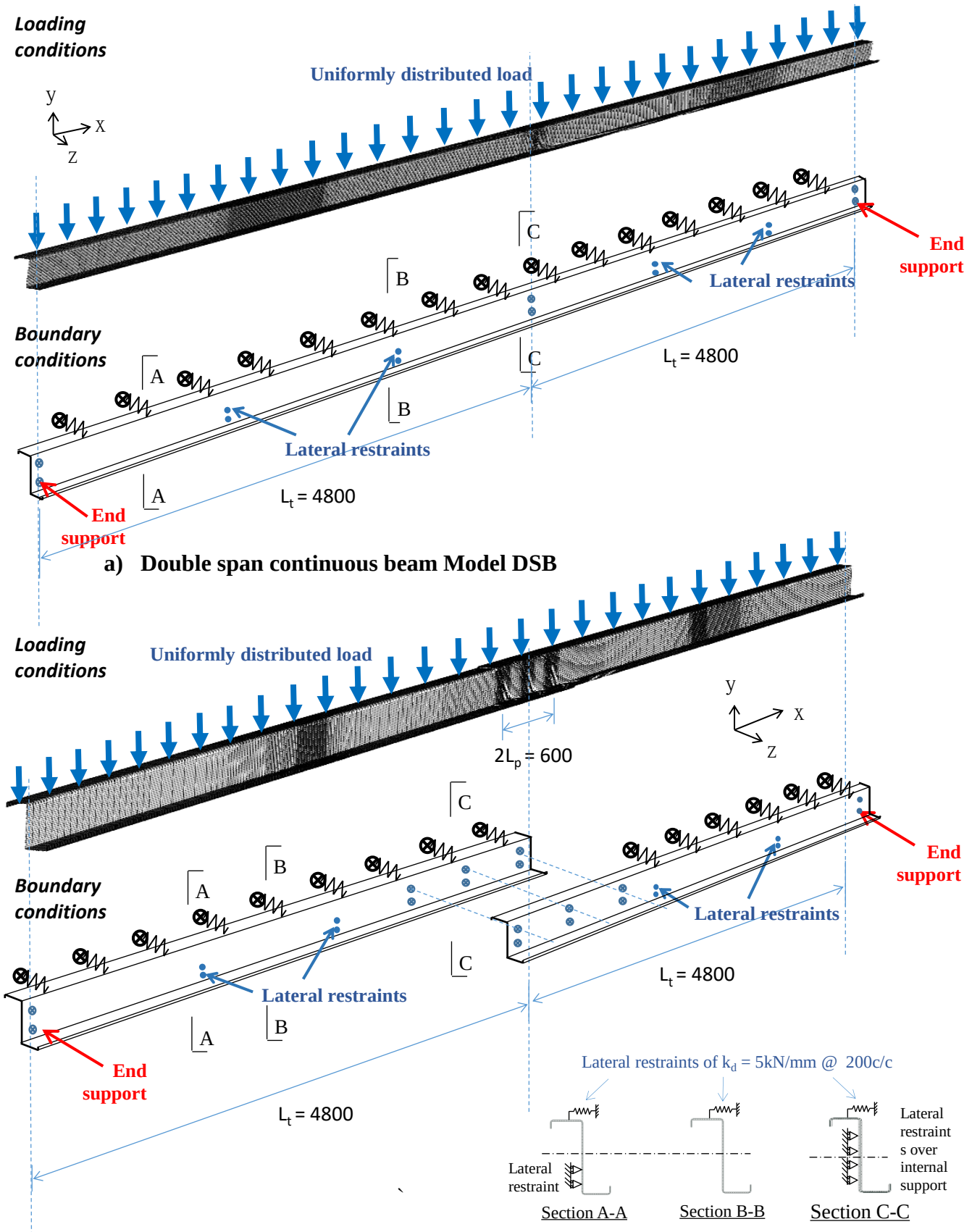

Figure 9. Double span beams

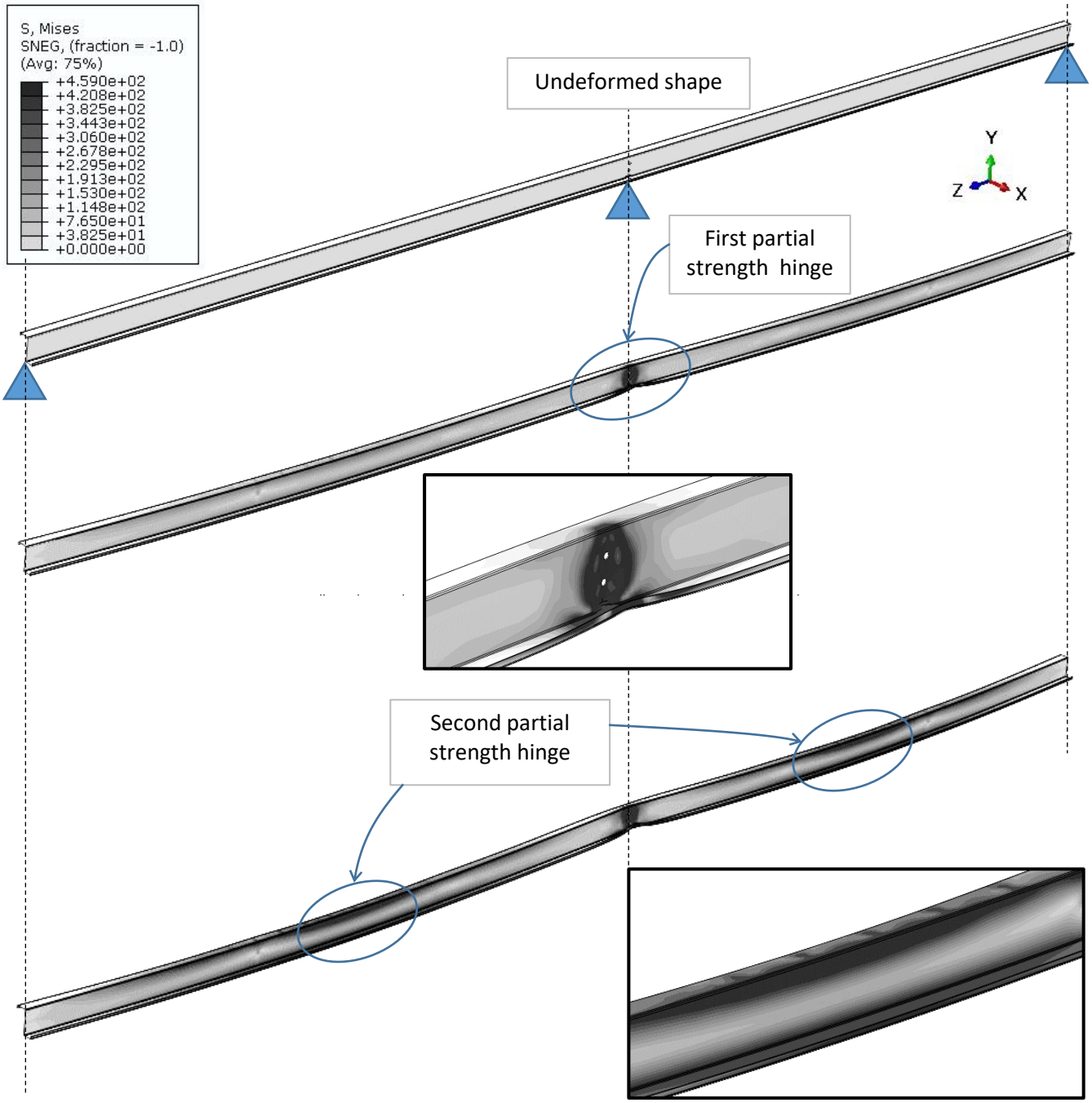

Figure 10. Deformed shape of Model DSB

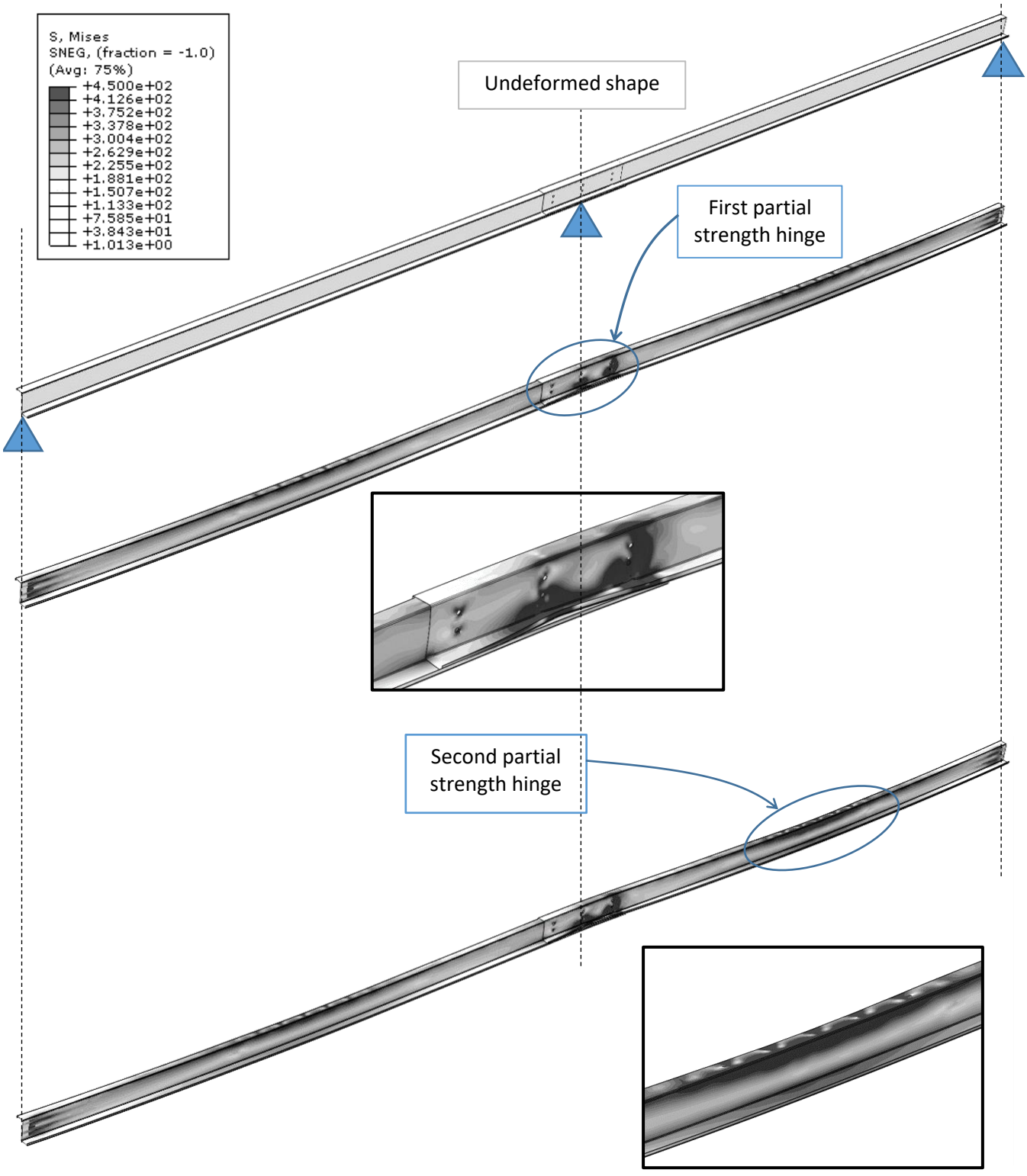

Figure 11. Deformed shape of Model DSB-4D

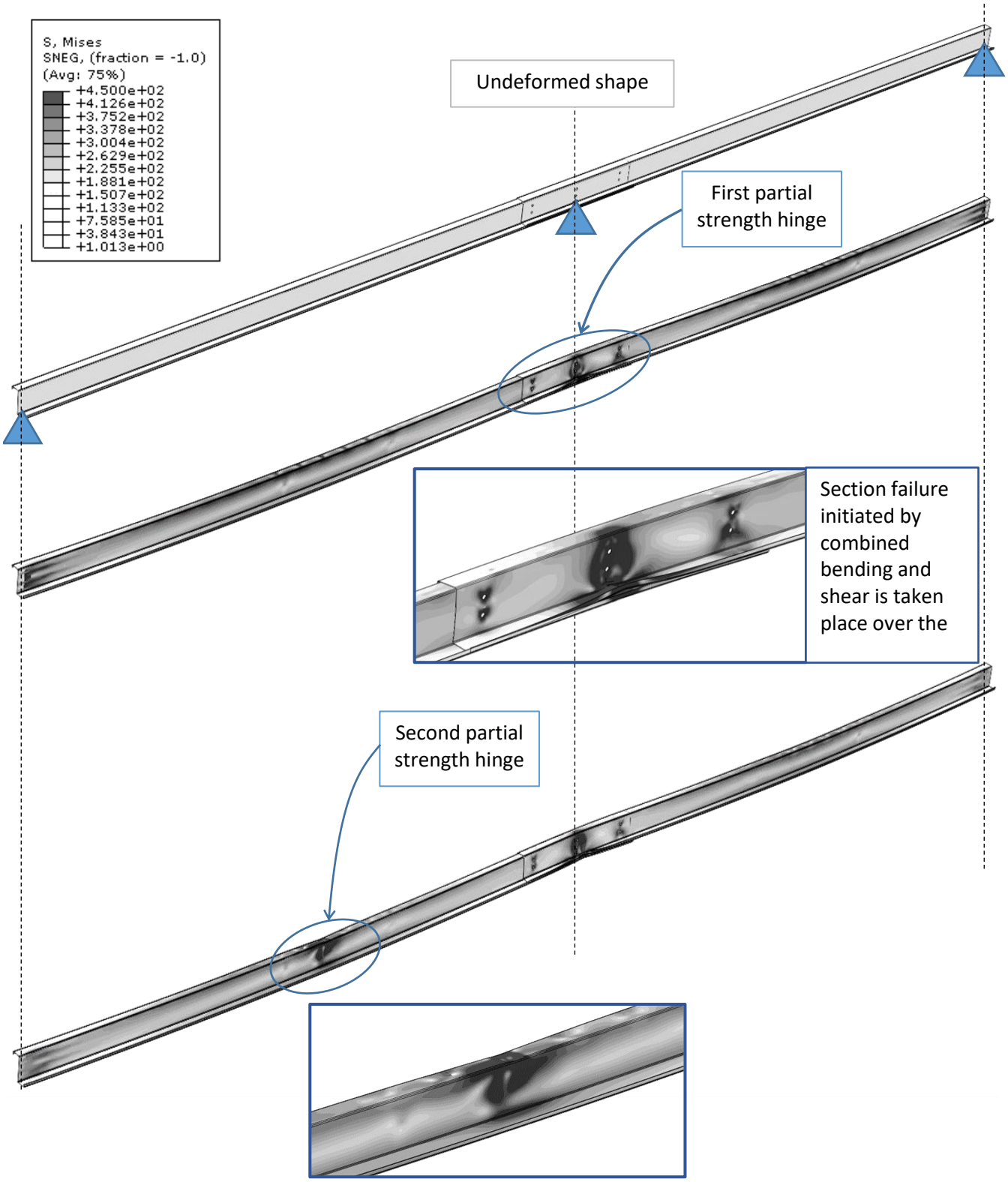

Figure 12. Deformed shape of Model DSB-6D

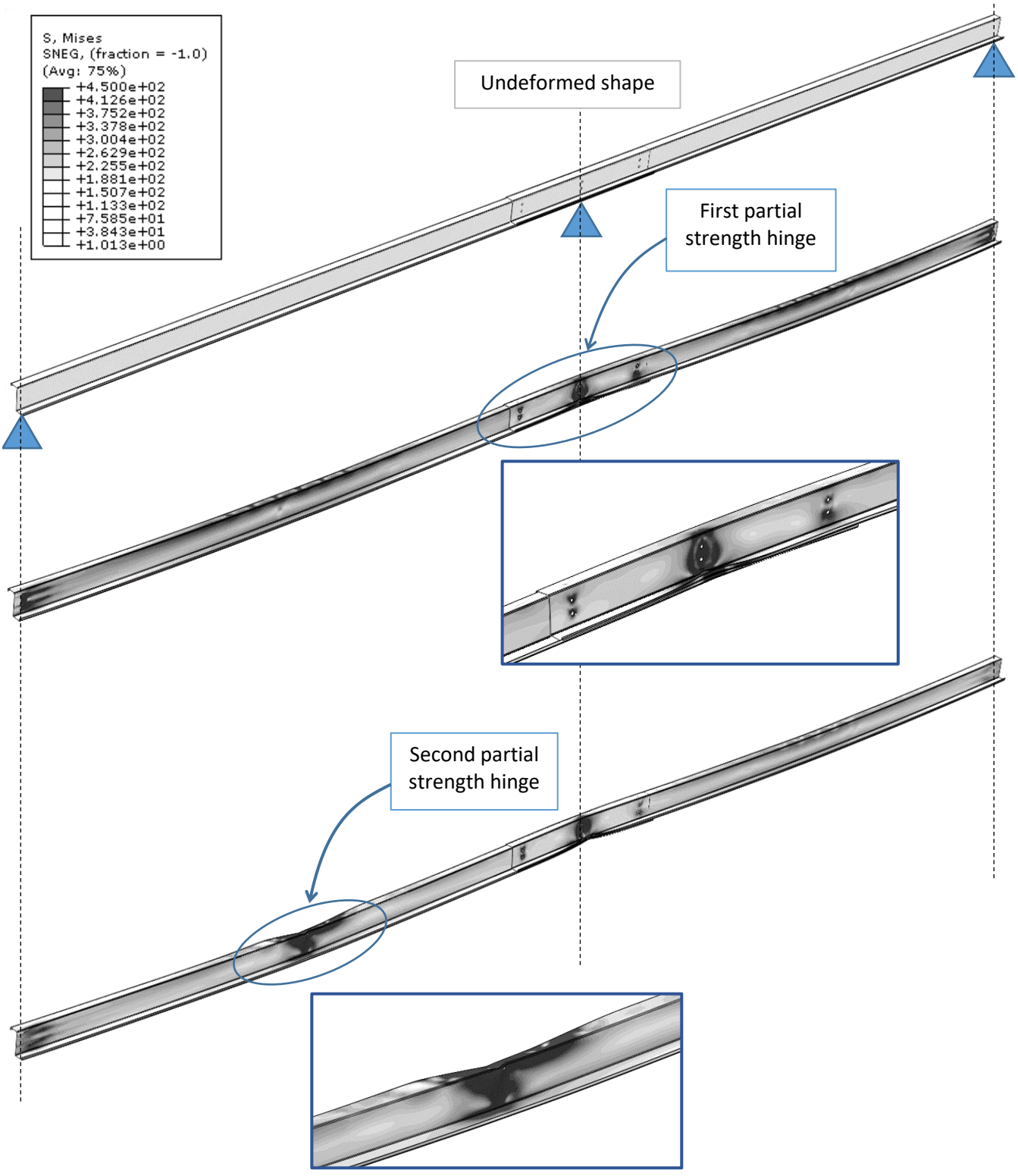

Figure 13. Deformed shape of Model DSB-8D

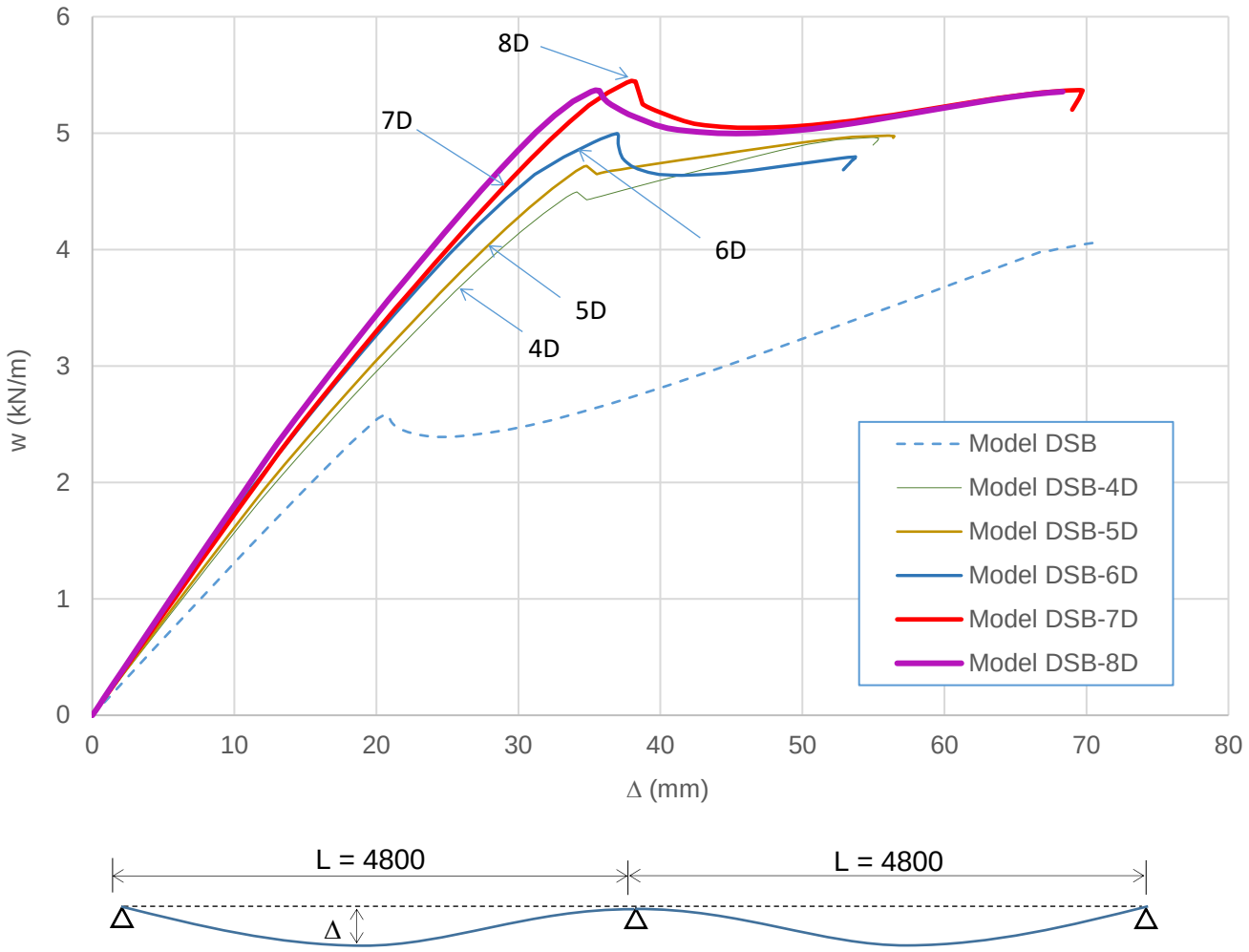

Figure 14. Load deflection curves of various models of double span beams

Table 1 Summary of test program and data

	Test	Test span L_t	Lap length $2L_p$	Section dimensions D	E	F	c	Bare metal thickness t	Measured yield strength p_y	Measured Young's Modulus E
		(mm)	(mm)	(mm)	(mm)	(mm)	(mm)	(mm)	(N/mm^2)	(kN/mm^2)
Z15016 G450	**ZACONR**	2550	-	150.7	67.4	63.5	16.5	1.65	541	199
	ZA018R	2550	180	151.0	67.4	63.5	16.5	1.67		
	ZA024R		240	151.0	67.7	63.4	16.6	1.65		
	ZA030R		300	151.0	67.7	63.4	16.6	1.65		
	ZA060R		600	150.9	67.6	63.5	16.4	1.66		
	ZA090R		900	150.7	67.5	63.1	16.6	1.65		

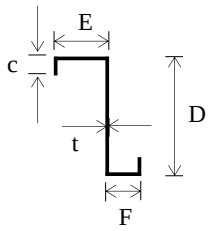

Table 2 Summary of test results

	Test	Test span L_t (mm)	Lap length $2L_p$ (mm)	Mode of failure*	Maximum applied load $2P_{max}$ (kN)	Maximum moment from test M_{test} (kNm)	Mid-span deflection Δ (mm)	Reference rotation θ (rad)
	ZACONR	2550	-	MV	31.91	10.17	17.9	0.014
Z15016 G450	**ZA018R**	2550	180	MV_e	27.95	8.91	37.1	0.029
	ZA024R		240		30.09	9.59	34.5	0.027
	ZA030R		300		33.88	10.80	30.6	0.024
	ZA060R		600		45.21	14.41	25.4	0.020
	ZA090R		900		50.98	16.25	23.1	0.018

*Notes:

MV denotes section failure of the Z-section under single point load.

MV_e denotes section failure at the single Z-section near the end of the lapped Z-sections under bending and shear.

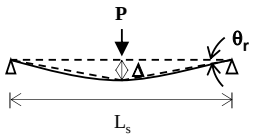

$\theta_r = 2 \times \Delta / L_s$

$M = PL_s / 4$

Table 3 Summary of numerical results

	Test	Test span L_t (mm)	Lap length 2 L_p (mm)	Failure mode*	Moment at mid-span, M_{test} (kNm)	Moment at mid-span, M_{FEM} (kNm)	Model factor $\frac{M_{test}}{M_{FEM}}$
	ZACONR	**2550**	**-**	MV	10.17	9.76	1.04
Z15016 G450	**ZA018R**	**2550**	180	MV_e	8.91	9.14	0.97
	ZA024R		240		9.59	9.55	1.00
	ZA030R		300		10.80	10.55	1.02
	ZA060R		600		14.41	13.60	1.06
	ZA090R		900		16.25	15.82	1.03

*Notes:

MV denotes section failure of the Z-section under single point load.

MV_e denotes section failure at the single Z-section near the end of the lapped Z-sections under combined and shear.

Table 4 Load resistances of various lapped double span beam models

Model	Formation of first hinge						Formation of second hinge			
	Applied load at first hinge w_1 (kN/m)	Reaction at end support R_{end} (kN)	Moment over internal support M_h (kNm)	Moment at end of lap M_e (kNm)	Moment at mid-span M_s (kNm)	Failure mode	Applied load at second hinge w_2 (kN/m)	Reaction at end support R_{end} (kN)	Moment over internal support M_h (kNm)	Moment at mid-span M_s (kNm)
DSB	2.59	4.46	-7.26	--	4.22	MV	4.12	8.92	-2.70	10.52
DSB-4D	4.49	8.61	-8.29	-8.81	9.09	MV_e	4.96	9.68	-8.32	10.40
DSB-6D	5.00	9.46	-8.90	-4.01	9.87	MV	4.79	10.03	-3.88	11.58
DSB-8D	4.71	8.75	-10.00	-2.81	8.91	MV	4.67	9.86	-4.27	11.21